

# Electronic properties of H on vicinal Pt surfaces: A first-principles study

T. Vehviläinen, P. Salo,\* and T. Ala-Nissila†

*Department of Applied Physics, Helsinki University of Technology,  
P.O. Box 1100, FI-02015 TKK, Espoo, Finland*

S.C. Ying

*Department of Physics, Brown University, Providence, Rhode Island 02912-1843*

(Dated: November 1, 2018)

In this work, we use the first-principle density-functional approach to study the electronic structure of a H atom adsorbed on the ideal Pt(111) and vicinal Pt(211) and Pt(331) surfaces. Full three-dimensional potential-energy surfaces (3D PES's) as well as local electronic density of states on various adsorption sites are obtained. The results show that the steps modify the PES considerably. The effect is nonlocal and extends into the region of the (111) terraces. We also find that different type of steps have different kind of influence on the PES when compared to the one of the ideal Pt(111) surface. The full 3D PES's calculated in this work provide a starting point for the theoretical study of vibrational and diffusive dynamics of H adatoms adsorbed on these vicinal surfaces.

PACS numbers: 68.43.Bc, 68.43.Fg, 71.15.Mb, 73.20.At

## I. INTRODUCTION

Systems in which hydrogen adatoms interact with transition metal surfaces have been intensively studied both experimentally and theoretically [1] since they have many important applications. For example, hydrogen adsorbed on platinum surfaces or on platinum nanoparticles constitutes an important application in catalysis of heterogeneous hydrogenation reactions, in the combustion of hydrocarbons, and in proton exchange membrane fuel cells.

On a more fundamental level, we need to understand basic dynamical properties of the adsorbed hydrogen such as vibrational excitations and diffusion coefficients in order to understand the chemical reactivity and catalytic activity on a more microscopic level. A particularly intriguing characteristic of H adatoms on metal surfaces is that they may exhibit distinct quantum-mechanical behavior at relatively high temperatures as compared to heavier elements or molecular adsorbates. In particular, H adatoms on metal surfaces can diffuse either through classical activated hopping or quantum-mechanical tunneling processes. At low enough temperatures many features of hydrogen diffusion on metal surfaces can only be explained by quantum effects, which are due to the small mass and delocalization of elemental H [1, 2, 3, 4, 5, 6, 7, 8, 9, 10, 11, 12].

The best studied system in this respect is H on Pt surfaces, as there have been a number of experimental and theoretical studies on the vibrational and diffusive dynamics of this system [8, 12, 13, 14, 15, 16, 17, 18, 19, 20, 21, 22, 23, 24, 25, 26, 27, 28, 29, 30, 31, 32,

33, 34, 35, 36, 37, 38, 39, 40, 41, 42, 43, 44]. Recently, the complete three-dimensional potential-energy surface (3D PES) for H/Pt(111) has been calculated from first-principles density-functional theory (DFT) approach. The vibrational excitations for this system are now well understood in terms of quantum transitions within a vibrational band structure [28, 29]. The experimental data for diffusion of H on Pt(111) are still controversial, as different techniques yield different results [21, 38, 42]. This can be qualitatively understood from the fact that the different techniques study the diffusion of H adatoms at different length scales. Thus, the influence of disorder plays a significantly different role in different experiments. This is particularly important in the low-temperature regime, where the quantum nature of H adatom motion is important. Here the role of disorder can lead to the localization of the wave-function of the H adatom that suppresses diffusion on a large length scale, such as in the optical diffraction grating experiments [6, 38, 42]. Again, for quantitative studies of diffusion, a necessary starting input is the microscopic PES and the ensuing vibrational band structures.

Realistic surfaces are hardly ever ideal and may contain defects such as isolated vacancies, dislocation lines or steps. On such surfaces, the defect sites are often catalytically very active. Stepped metal surfaces with a regular step spacing can be easily prepared by cutting a single crystal in a direction vicinal to a high-symmetry plane. Hydrogen on stepped platinum surfaces has been studied [35, 36, 37, 38, 39, 40, 41, 42, 43, 44] as the presence of step edges increases the dissociation and sticking of hydrogen [14]. For instance, Gee *et al.* [35] have suggested that step sites are responsible for the low-energy dissociative adsorption of H<sub>2</sub> and the high-energy dissociation of H<sub>2</sub> is associated with the (111) terrace sites on the Pt(533) surface. McCormack *et al.* [40] carried out density-functional calculations to study the dissociative adsorption of H<sub>2</sub> on the Pt(211) surface, and their

---

\*Electronic address: Petri.Salo@tkk.fi

†Also at Department of Physics, Brown University, Providence, Rhode Island 02912-1843

results are in good agreement with the experiment results for  $H_2$  on Pt(533) [35]. Recently, Olsen *et al.* [43] have studied  $H_2$  dissociation on the Pt(211) stepped surface using quantum-dynamics calculations. Their results show enhancement of dissociation at low collision energies in qualitative accordance with recent experiments [44].

Zheng *et al.* [38, 42] have studied diffusion dynamics of H on stepped Pt(111) surfaces experimentally using a linear optical diffraction technique. They found faster diffusion perpendicular to the steps than that on a flat Pt(111) surface [38]. This cannot be explained within the lattice gas model indicating that the effect of steps have to be nonlocal in the sense that it extends to the terrace sites. Motivated by this result, in this work we study the electronic properties of a hydrogen atom, in particular the PES of H adsorbed on the vicinal Pt(211) and Pt(331) surfaces using DFT calculations. We calculate the full 3D PES for the two vicinal surfaces and present a comprehensive comparison between the two types of steps on the H/Pt(111) system. The results show that the steps indeed modify the PES considerably even in the region of (111) terraces and the different type of steps have different kind of effect on the PES when compared to the PES of the flat Pt(111) surface. The PES's obtained can be used in the future to study the effect of steps *e.g.* on the vibrational band structure, and classical and quantum diffusion of H on vicinal Pt surfaces.

This paper is organized as follows. In Section II we describe the computational details, in Section III we present the results and discuss the influence of steps on the behavior of H on Pt surfaces, and finally in Section IV we give some concluding remarks based on the results obtained.

## II. METHODS

We have done the DFT calculations using the Vienna *Ab-initio* Simulation Package (VASP) [45] with the generalized-gradient approximation (GGA) of PW91 [46] and with projector-augmented wave (PAW) potentials [47]. The cutoff energy for the plane-wave expansion is 450 eV. For the irreducible Brillouin-zone integration we use Monkhorst-Pack [48]  $13 \times 13 \times 1$   $\mathbf{k}$ -point sampling for Pt(111) and  $6 \times 6 \times 1$  mesh for Pt(211) and Pt(331), together with a smearing of 0.2 eV for the Methfessel-Paxton occupation function which significantly shortens the computing time for transition metal compared to other existing methods [49]. The energy convergence with respect to the  $\mathbf{k}$ -points and cutoff energy has been tested and based on these tests the estimated accuracy of the energies is of the order of 0.01 eV and the accuracy of structures is within 0.01 Å. On the other hand, the error due to the choice of the GGA etc. is about 0.02 eV as will be shown in the case of H on Pt(111) later on.

The crystal structure of Pt is face-centered cubic (fcc) and the calculated lattice constant of Pt is 3.987 Å, the

experimental value being 3.924 Å [50]. We use a supercell which consists of 4, 12 and 11 atomic layers, corresponding 4, 36 and 33 atoms in the supercell for the Pt(111), Pt(211), and Pt(331) systems, respectively. Thus, the surface unit cell consists of  $1 \times 1$  atom for the Pt(111) surface and  $3 \times 3$  atoms for the Pt(211) and Pt(331) surfaces. The distance between the slabs is at least 12 Å which is sufficient to eliminate the interaction between them.

Two hydrogen atoms form a  $H_2$  molecule whose calculated bond length is 0.75 Å and binding energy  $E_{bin} = E_{H_2} - 2E_H = -4.55$  eV. These values are in an excellent agreement with experimental values [51]. Based on the data for the energy *vs.* bond length of a hydrogen molecule we can say that H atoms do not interact with each other if the distance between them is over 7 Å (see [52]). When we construct our Pt(211) and Pt(331) supercells such that the H-H distance is larger than this value we study effectively a single H atom interacting with the surface. This is very important since the H-H interaction can significantly influence the energy of the saddle point [38]. In our calculations, the distance between the H atoms on the same (111) terrace, but in different supercells, is 8.46 Å.

In the slab relaxation the bottom-most layer is fixed in the Pt(111) calculations and in the Pt(211) and Pt(331) calculations six bottom layers are fixed to the bulk coordinates. After the relaxation all the Pt atom positions are fixed and no Pt atom movements are allowed during the calculations for the hydrogen atom on a surface. The relaxations of Pt atoms due to H are small and can therefore be neglected [28].

Both the (211) and (331) vicinal surfaces consist of three-atoms wide fcc(111) terraces. These vicinal surfaces have different atomistic structures at the step edges. The step is called an *A-type* step if the orientation of the step is (100) and a *B-type* step if the orientation is (111). The ideal positions of the atoms for the (211) and (331) surfaces are schematically shown in Fig. 1.

## III. RESULTS AND DISCUSSION

### A. Potential-Energy Surfaces

We have calculated three-dimensional adiabatic potential-energy surfaces (3D APES) for H on Pt(111), Pt(211) and Pt(331). The total energy for H on Pt has been calculated in a grid on each surface and at each site with different heights ( $z$ ) around the minimum position. The Morse potential [53] fitted to the data is of the form

$$U(x, y, z) = A(x, y) \left\{ 1 - e^{-B(x, y)[z - C(x, y)]} \right\}^2 + D(x, y),$$

where  $A$ ,  $B$ ,  $C$  and  $D$  are fitting parameters that depend on the position  $(x, y)$ . This potential form works well when the height from the surface is over 0.3 Å. Under this limit the potential is overestimated near the fcc and hcp

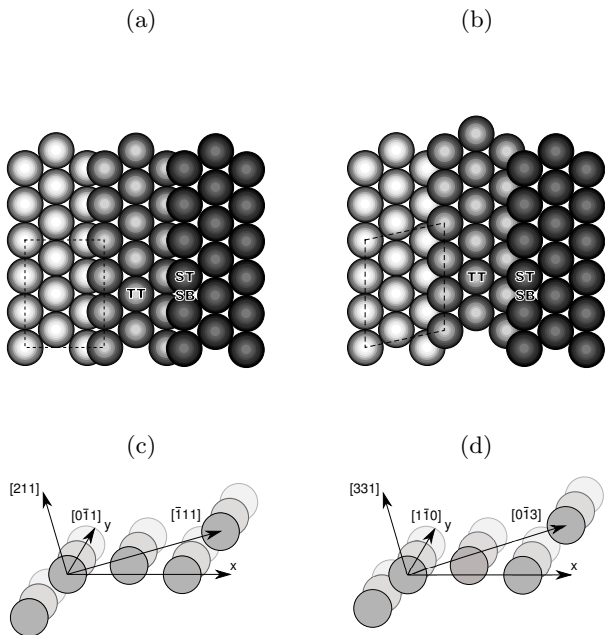


FIG. 1: Top view of (a) Pt(211) and (b) Pt(331) surfaces. Terraces are both fcc(111), but the step edge of Pt(211) is fcc(100) (*A* type) while the one for Pt(331) is fcc(111) (*B* type). The surface supercells used in the calculations are shown with dashes lines. The most stable adsorption sites for H are also shown: terrace-top (TT), step-top (ST), and step-bridge (SB) site. Side view of (c) Pt(211) and (d) Pt(331) surfaces with corresponding lattice directions in the supercells. In addition, the *y* axis is along the step edge and *x* axis along the terrace and perpendicular to the step edge, *i.e.* *x* points to  $\overline{2}11$  in (c) and to  $\overline{1}12$  in (d).

sites. However, by studying wave functions and eigenvalues of the H atom on Pt(111) [8, 27, 29], we conclude that it is adequate to calculate the potential accurately using a dense grid near the minimum at each  $(x, y)$  site and elsewhere use a coarse grid and a feasible approximation for the potential.

### 1. H on the Flat Pt(111) Surface

A full monolayer (1.0 ML) of H on Pt(111) has been calculated to test that our present results are consistent with previous DFT calculations. Also, the data for H on the flat Pt(111) surface is needed to be able to see how a step changes the electronic structure seen by the H atom. Even though the activation energy for H diffusion depends on the H coverage [38], the 2D APES of H on Pt(111) with 0.25 and 1.0 ML are qualitatively similar [54], thus we can use the present 1.0 ML data for H/Pt(111) when compared the qualitative changes due to the step in the 2D APES of H on stepped Pt(111) surfaces.

In Fig. 2(a) we show the calculation grid with a total

number of 36 equidistant positions on the  $(x, y)$  plane over the surface. For each of these positions the total energy of the system has been calculated using various *z* values around the minimum position, the total number of calculated points being 219. The minimum energy 2D APES is shown in Fig. 2(a), the total energy of the system with H at different heights, *i.e.* *z* positions around the minimum along the path from an fcc to top site in Fig. 2(b), and the minimum energy and height of H along the path top–fcc–hcp–top are presented in Fig. 2(c).

In Table I, the adsorption energy of the H atom at different sites on the Pt(111) surface, the energy differences for H to move from a site to another (see also Fig. 2(c)), and calculated vibrational energies based on the harmonic approximation for perpendicular ( $\hbar\omega_{\perp}$ ) and parallel motion ( $\hbar\omega_{\parallel}$ ) are presented. The calculated energies represented in Table I and the energy profile of the 2D APES along the path top–fcc–hcp–top for H on Pt(111) shown in Fig. 2(c) can be compared to those calculated by Bădescu *et al.* [29] and Olsen *et al.* [22]. The curvature and shape of the energy profile are very similar compared to those of Bădescu *et al.* The only major difference is the top site where the energy is much higher in the present study. However, it is highly unlikely that H is adsorbed at the top site [29] and thus one cannot resolve further the energy of H at the top site based on the experiments. To check the accuracy numerically we made some test calculations with a different GGA (PBE [55]), potential (ultrasoft pseudopotential [56]) and Fermi smearing method. The difference between the energies of H at the fcc and hcp sites is hardly affected at all, the difference in all the cases being 0.07 eV, while there are some variations in the energy difference between fcc and top. With PBE GGA the energy difference between H on Pt(111) at the fcc and top sites is 0.10 eV, with ultrasoft pseudopotential 0.11 eV, and with Fermi smearing it is 0.08 eV, the energy difference with PW91 GGA being 0.09 eV (Table I). Thus, the error due to different methods is about 0.02 eV and the present results seem to be quite accurate.

There are more differences in the energy profile when compared to that of Olsen *et al.* [22]. Nevertheless, the vibrational energies based on the harmonic approximation are in a good agreement both with the results by Olsen *et al.* [22] and Bădescu *et al.* [29]. This indicates similar curvature and shape of the 2D potential-energy surfaces for H at the high-symmetry sites on Pt(111).

### 2. H on the Vicinal Pt(211) and Pt(331) Surfaces

The 3D APES's of H on Pt(211) and Pt(331) have been calculated using a grid consisting of 30 positions for H on Pt(211) and 25 positions for H on Pt(331) on the  $(x, y)$  plane over the surface. The grids are constructed so that there is a grid point at every high-symmetry site (fcc, hcp, top and bridge) and at least one midpoint between these sites. This assures that the adsorption energy at

TABLE I: H on Pt(111). Adsorption energy  $E_{ads}$ , activation energy  $\Delta E$  (in parenthesis the site towards which the barrier is represented), harmonic vibrational energies  $E_{vib}^{\perp}$  and  $E_{vib}^{\parallel}$  along directions  $[hkl]$ . All data in eV.

site	$E_{ads}$	$\Delta E$ (neighboring site)		$E_{vib}^{\perp}[111]$	$E_{vib}^{\parallel}[\bar{1}10]$	$E_{vib}^{\parallel}[\bar{1}12]$
top	-0.33	0.090 (fcc)	0.120 (hcp)	0.277	0.066	0.033
hcp	-0.35	0.035 (fcc)	0.140 (top)	0.144	0.099	0.028
fcc	-0.42	0.200 (top)	0.103 (hcp)	0.143	0.082	0.082

TABLE II: H on Pt(211). Adsorption energy  $E_{ads}$ , harmonic vibrational energies  $E_{vib}^{\perp}$  and  $E_{vib}^{\parallel}$  along directions  $[hkl]$ . All data in eV.

site	$E_{ads}$	$E_{vib}^{\perp}[211]$	$E_{vib}^{\parallel}[\bar{1}11]$	$E_{vib}^{\parallel}[\bar{0}\bar{1}1]$
step-top	-0.44	0.269	0.048	0.046
step-bridge	-0.59	0.160	0.069	0.126
terrace-top	-0.38	0.268	0.088	0.048

each local minimum site is calculated and also the energy barrier between these sites is calculated with a reasonable accuracy. The grids used in the calculations are shown in Figs. 3(a) and 4(a). The total energy of the system has been calculated at each surface site using various  $z$  values. The number of calculated  $z$  values is 7 – 10 at terrace sites and 20 – 30 at sites near the step edge. This difference is due to the shape of the potential. At terrace sites the geometry of the potential is similar to that of the Morse potential and the number of calculated points can be small, but near the step edge the shape is more complicated due the interaction between the H atom and step atoms, and thus a denser grid along the  $z$  direction near the step region is needed.

The calculated 2D APES's of H on Pt(211) and Pt(331) are also shown in Figs. 3(a) and 4(a), respectively. There are three energy minima for H on the Pt(211) and Pt(331) surfaces. The deepest minimum is between two step-edge atoms (*step-bridge site*) for both the Pt(211) and Pt(331) surfaces. The other two minima are above a terrace atom (*terrace-top site*) and above a step-edge atom (*step-top site*).

The values of the adsorption and harmonic vibrational energies for H on Pt(211) and Pt (331) are shown in Tables II and III, respectively. There are only minor changes for the perpendicular vibrational energies; it is mainly the parallel vibrational models that are affected by the steps. On the other hand, when we compare these 2D APES plots to the 2D APES plot for H on the ideal Pt(111) surface, one cannot see any similarities in the (111) terrace region. The step thus influences the adsorption everywhere in the three-atom wide terrace region.

The calculated 2D APES for H on Pt(211) can be compared to the one calculated by Olsen *et al.* [36]. These two are in close agreement and the differences can be explained with different computational parameters and interpolation methods. Also, the calculation grid used in the present work is denser than the grid used by Olsen

TABLE III: H on Pt(331). Adsorption energy  $E_{ads}$ , harmonic vibrational energies  $E_{vib}^{\perp}$  and  $E_{vib}^{\parallel}$  along directions  $[hkl]$ . All data in eV. Direction  $[\bar{1}\bar{1}6]$  is along the (331) surface and perpendicular to the step-edge direction  $[1\bar{1}0]$ . See also Fig. 1.

site	$E_{ads}$	$E_{vib}^{\perp}[331]$	$E_{vib}^{\parallel}[\bar{1}\bar{1}6]$	$E_{vib}^{\parallel}[1\bar{1}0]$
step-top	-0.37	0.268	0.039	0.051
step-bridge	-0.41	0.162	0.046	0.120
terrace-top	-0.36	0.265	0.096	0.061

*et al.*

The effect of the step edge can also be seen in the behavior of the total energy as a function of the height of H from the surface near the step edge. The calculated total energy of H on stepped Pt surfaces at selected positions (for more data see the web link in Ref. [52]) as a function of the height  $z$  from the surface is plotted in Figs. 3(b) and 4(b). Near the step edge the potential has a double-well structure not seen in the 2D APES's, but which can be seen when the height of the H atom is modified. When the H atom is far away from the step edge the shape of the potential in the  $z$  direction is of the Morse potential form. The double well structure of the potential exists near the step region and it is due the interaction between the step atoms and the H atom. It is also clear that there are significant quantitative differences between the full 3D APES of the (211) and (331) surfaces. For example, the  $z$  positions and the curvatures of the minima differ dramatically. Such differences in the APES lead into large differences in the vibrational band structure of H adatoms on these surfaces, which indicates significantly different behavior for quantum diffusion of H at low temperatures.

The minimum-energy paths (MEP) for H moving from a lower terrace to an upper one were calculated using the nudged elastic band (NEB) method [57] with which one can find (local) minimum path for transition between two local minimum configurations. The corresponding classical diffusion paths for H on Pt(211) and Pt(331) are presented in Figs. 3(a) and 4(a), respectively. The corresponding energy values and the distance of the H from the surface are presented in Figs. 3(c) and 4(c), respectively. In these plots one can see a potential barrier when H approaches the step. This barrier is located before the step edge of the upper terrace and before the formation of the double-well potential. The energy barriers between two step-bridge minima are 0.30 and 0.29 eV for the activated

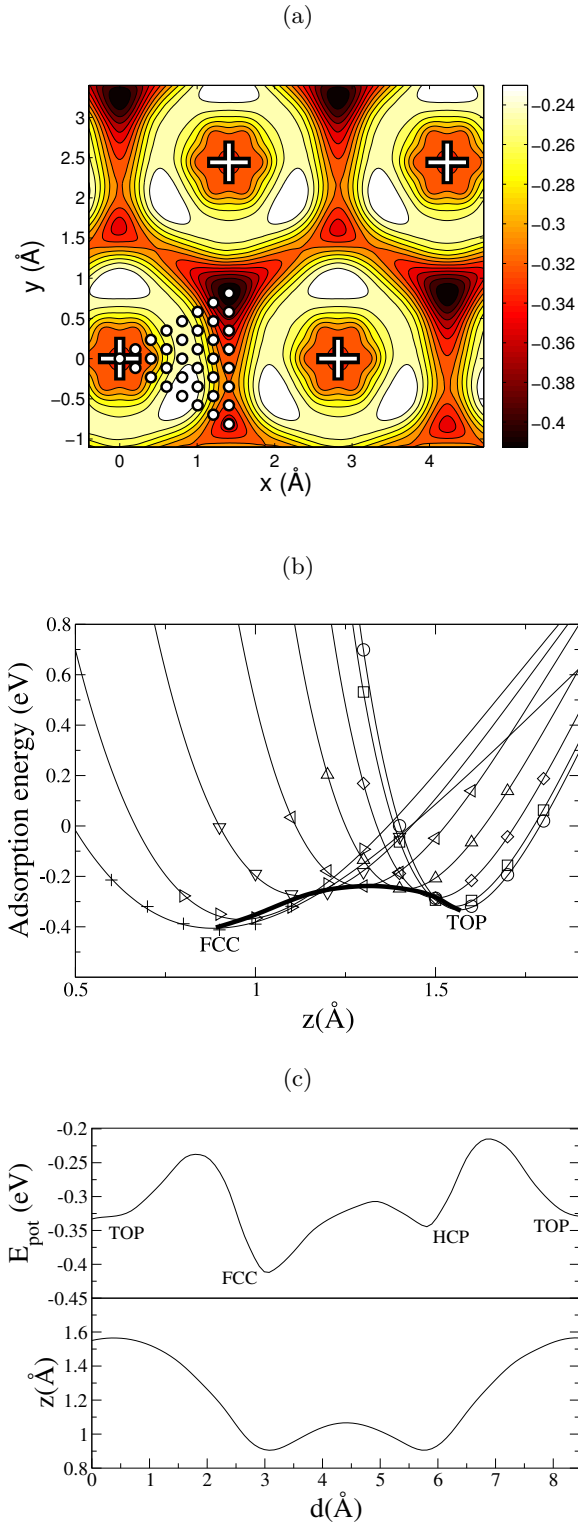


FIG. 2: Results for H on Pt(111). (a) (Color online) Minimum energy 2D APES for H on Pt(111) (in eV). Crosses represent the positions of surface Pt atoms and open dots the grid points used in the calculations. The  $x$  and  $y$  axis corresponds to  $\overline{[110]}$  and  $\overline{[1\bar{1}2]}$  directions, respectively. (b) Energy for different  $z$  positions around the minimum along the path from an fcc to top site. (c) Minimum energy and height of H along the path top-fcc-hcp-top as a function of the distance  $d$  along the path.

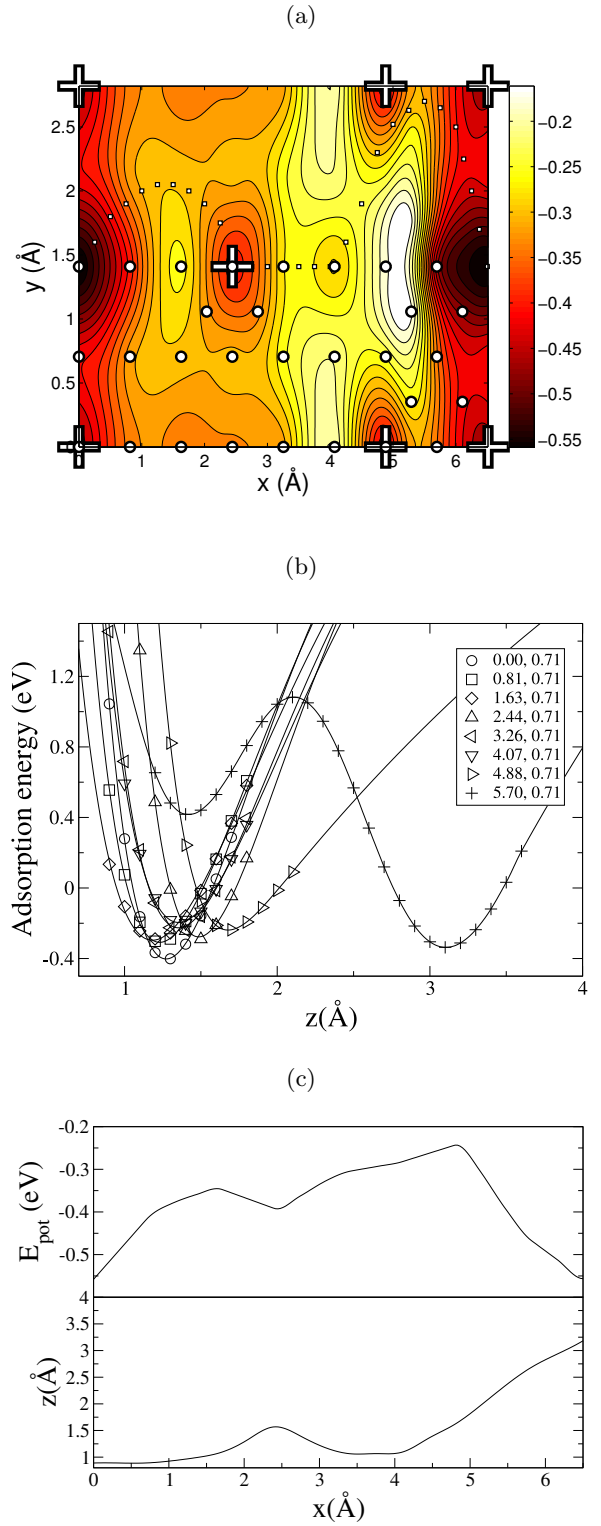


FIG. 3: Results for H on Pt(211). (a) (Color online) Minimum energy 2D APES for H on the surface (in eV). Crosses represent the positions of surface Pt atoms such that the two right-most atoms are the edge atoms on the upper terrace, the other ones residing on the lower terrace. Open dots are the grid points used in the calculations. Small open squares represent the minimum energy path across the surface perpendicular to the step edge. (b) Energy for different  $z$  positions around the minimum along the path whose coordinates (Å) are included in the insert. (c) Minimum energy profile and height of H along the minimum energy path shown in (a).

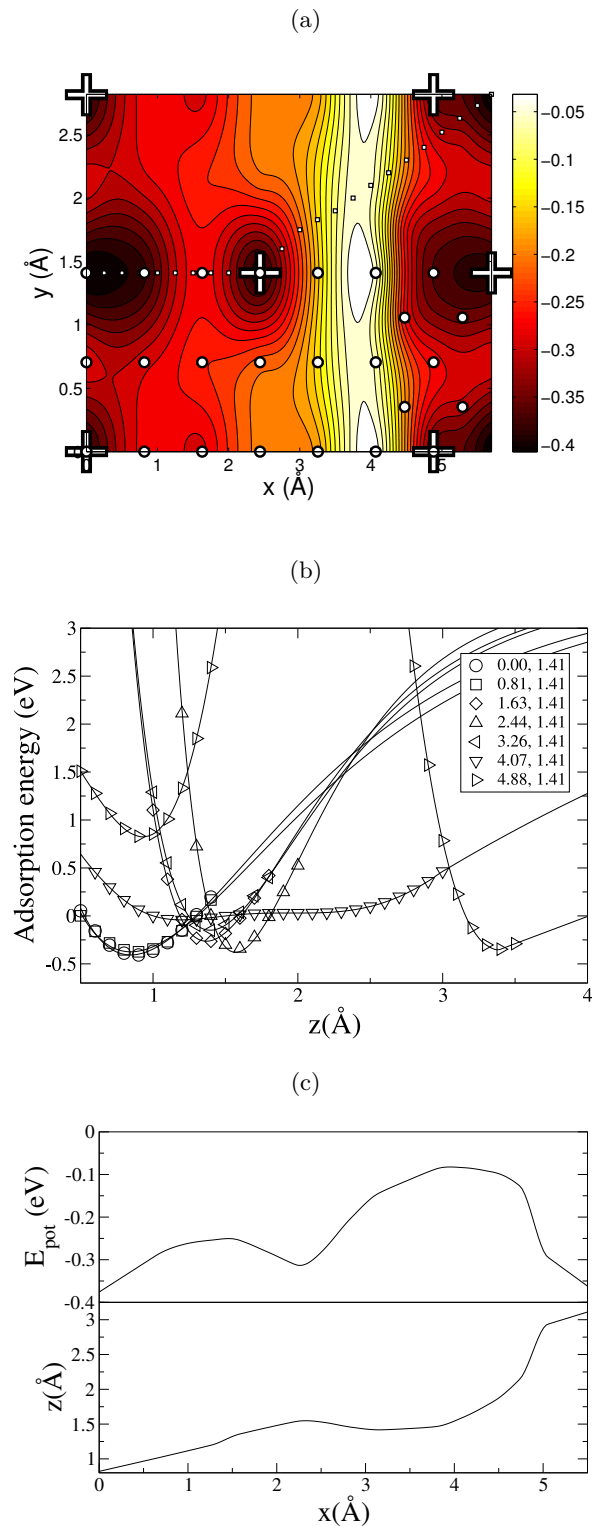


FIG. 4: Results for H on Pt(331). See details in the caption of Fig. 3. *N.B.* In (a) the Pt atom at (0, 0) corresponds to the one on the upper terrace at (5.69, 1.41). See also Fig. 1(b).

diffusion of H on the Pt(211) and Pt(331) surfaces, respectively. On the other hand, the energy barriers along the step edges are lower, being only 0.15 and 0.11 eV for H on the Pt(211) and Pt(331) surfaces, respectively.

## B. Local Density of States

To understand better the bonding between the H atom and Pt surface atoms we have calculated the local density of states (LDOS) for H at selected minimum energy sites and for the nearest Pt atoms and projected them onto the states of the chosen angular momentum. The Wigner-Seitz radii used for H and Pt atoms are 0.370 Å and 1.455 Å, respectively. An extensive set of calculated LDOS's can be found on the web page in Ref. [52].

There are three minimum energy sites for H on the Pt(111) surface, *i.e.* fcc, hcp and top. LDOS's have been calculated at each of these sites for H and the nearest Pt atom of H [52]. For H adsorbed at the top site the 1s orbital of H and  $5d_{z^2}$  of Pt hybridize in the energy range of  $[-7 \text{ eV}, -3 \text{ eV}]$  (see Fig. 5(a)). The adsorption of H at the fcc and hcp hollow sites is similar, but considerably different from the adsorption of H at the top site [52]. For H at the fcc and hcp sites, new peaks appear in LDOS's between  $[-8 \text{ eV}, -7 \text{ eV}]$ . These LDOS's show hybridization of the 1s orbital of H and the 6s and  $5d_{xy}$  orbitals of Pt. Hong *et al.* [33] and Légaré [30] have calculated LDOS for H interacting with Pt(111) surface and our results are in a good agreement with their results.

On the vicinal surfaces, there are three energy minima for H on Pt(211) and Pt(331). The deepest minimum is at the step-bridge site while the other two minima are at the terrace-top and step-top sites. In Fig. 5 we show a series of LDOS's for the flat (111) and vicinal surfaces for the top and terrace-top site, respectively. It can be clearly seen in Fig. 5 that the steps influence the H and Pt  $s$  orbitals relatively little. However, there are significant differences between the more localized  $d$  orbitals of the Pt surface atoms. This indicates the non-local nature of the influence of the steps even on the terrace atoms on vicinal surfaces. Further analysis of the LDOS curves indicates that for terrace-top and step-top sites there is hybridization between the 1s orbital of H and the  $5d_{z^2}$  orbital of Pt as on the Pt(111) surface when H is adsorbed at the top site. When H is adsorbed at the step-bridge site the bonding and electronic structure are different. LDOS shows strong hybridization between the 1s orbital of H and the 6s,  $5d_{xz}$  and  $5d_{x^2-y^2}$  orbitals of the step-edge Pt atom. Thus, despite the geometric differences between the  $A$  and  $B$  type of steps, the binding of H to the Pt atoms on the surfaces seems to be similar.

## IV. SUMMARY AND CONCLUSIONS

In this work, we have used the first-principles DFT approach to study the electronic structure of H adsorbed

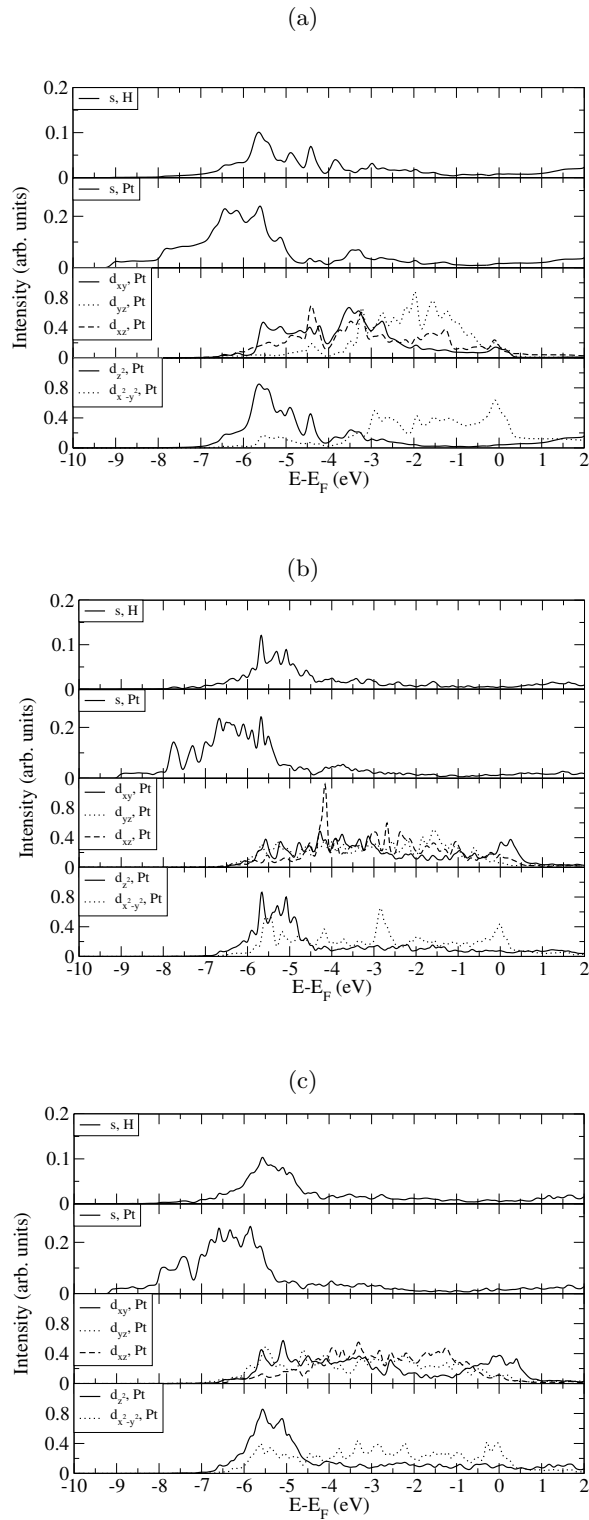


FIG. 5: LDOS curves for H on Pt surfaces: H at (a) the top site on Pt(111), (b) the terrace-top site on Pt(211), and (c) the terrace-top site on Pt(331).

on the vicinal Pt(211) and Pt(331) surfaces. We have evaluated the full 3D potential-energy surface for the adsorbed hydrogen. We have also studied the local density of states for the adsorbed hydrogen at various sites which provides a more detailed look at the changes in electronic structure due to the adsorption of hydrogen at various substrate sites. We have found that the preferred adsorption (minimum energy) site for H on Pt surfaces is the fcc site on the Pt(111) surface and the step-bridge site, *i.e.* the site between two step atoms, on the Pt(211) and Pt(331) surfaces. The step edge on Pt surfaces changes the potential-energy surface for H on the three-atoms wide (111) terrace quite dramatically when compared to the case of the flat Pt(111) surface. This is in qualitative agreement with the experimental observation that the step effect on the electronic structure is nonlocal and extends far beyond to the terrace location [38]. For instance, near the step edge the potential has a double-well structure which is due to the interaction between the H atom and Pt atoms of the step edge. Even though the adsorption energies and the density of states as well as the vibrational energies based on the harmonic approximation are quite similar for the H on the Pt(211) and Pt(331) surfaces at the corresponding adsorption sites, the anharmonic effects, for instance, can contribute quite dramatically to the vibrational band structure and also to the nature of diffusion of H on stepped surfaces. The calculated 3D APES provides a necessary input for further studies of vibrational and diffusive dynamics of H adatoms on the vicinal surfaces of Pt.

## Acknowledgements

This work has been in part supported by the Academy of Finland through its Center of Excellence program (COMP). We greatly acknowledge generous computing resources provided by the Finnish IT Center for Science (CSC).

- 
- [1] M. Nishijima, H. Okuyama, N. Takagi, T. Aruga, and W. Brenig, *Surf. Sci. Rep.* **57**, 113 (2005).
- [2] K. Christmann, R.J. Behm, G. Ertl, M.A. Van Hove, and W.H. Weinberg, *J. Chem. Phys.* **70**, 4168 (1979).
- [3] M.J. Puska, R.M. Nieminen, M. Manninen, B. Chakraborty, S. Holloway, and J.K. Nørskov, *Phys. Rev. Lett.* **51**, 1081 (1983).
- [4] M.J. Puska and R.M. Nieminen, *Surf. Sci.* **157**, 413 (1985).
- [5] E.A. Daniels and R. Gomer, *Surf. Sci.* **336**, 245 (1995).
- [6] G.X. Cao, E. Nabighian, and X.D. Zhu, *Phys. Rev. Lett.* **79**, 3696 (1997).
- [7] L.J. Lauhon and W. Ho, *Phys. Rev. Lett.* **85**, 4566 (2000).
- [8] K. Nobuhara, H. Nakanishi, H. Kasai, and A. Okiji, *Surf. Sci.* **493**, 271 (2001).
- [9] S.C. Badescu, S.C. Ying, and T. Ala-Nissila, *Phys. Rev. Lett.* **86**, 5092 (2001).
- [10] P.G. Sundell and G. Wahnström, *Phys. Rev. Lett.* **92**, 155901 (2004); *Phys. Rev. B* **70**, 081403(R) (2004); *Surf. Sci.* **593**, 102 (2005).
- [11] M. Leino, J. Nieminen, and T.T. Rantala, *Surf. Sci.* **600**, 1860 (2006).
- [12] T. Roman, H. Nakanishi, W.A. Diño, and H. Kasai, *e-J. Surf. Sci. Nanotech.* **4**, 619 (2006).
- [13] K. Christmann, G. Ertl, and T. Pignet, *Surf. Sci.* **54**, 365 (1976).
- [14] K. Christmann and G. Ertl, *Surf. Sci.* **60**, 365 (1976).
- [15] A.M. Baró, H. Ibach, and H.D. Bruchmann, *Surf. Sci.* **88**, 384 (1979).
- [16] L.J. Richter and W. Ho, *Phys. Rev. B* **36**, 9797 (1987).
- [17] P.J. Feibelman and D.R. Hamann, *Surf. Sci.* **182**, 411 (1987).
- [18] W. Di, K.E. Smith, and S.D. Kevan, *Phys. Rev. B* **45**, 3652 (1992).
- [19] P.J. Feibelman, *Phys. Rev. B* **56**, 2175 (1997).
- [20] S. Horch, H.T. Lorensen, S. Helveg, E. Laegsgaard, I. Stensgaard, K.W. Jacobsen, J.K. Nørskov, and F. Besenbacher, *Nature* **398**, 134, March (1999).
- [21] A.P. Graham, A. Menzel, and J.P. Toennies, *J. Chem. Phys.* **111**, 1676 (1999).
- [22] R.A. Olsen, G.J. Kroes, and E.J. Baerends, *J. Chem. Phys.* **111**, 11155 (1999).
- [23] E. Pijper, G.J. Kroes, R.A. Olsen, and E.J. Baerends, *J. Chem. Phys.* **113**, 8300 (2000).
- [24] K. Nobuhara, H. Nakanishi, H. Kasai, and A. Okiji, *J. Appl. Phys.* **88**, 6897 (2000).
- [25] G. Papoian, J.K. Nørskov, and R. Hoffmann, *J. Am. Chem. Soc.* **122**, 4129 (2000).
- [26] G.W. Watson, R.P.K. Wells, D.J. Willock, and G.J. Hutchings, *J. Phys. Chem. B* **105**, 4889 (2001).
- [27] G. Källén and G. Wahnström, *Phys. Rev. B* **65**, 033406 (2001).
- [28] Ş.C. Bădescu, P. Salo, T. Ala-Nissila, S.C. Ying, K. Jacobi, Y. Wang, K. Bedürftig, and G. Ertl, *Phys. Rev. Lett.* **88**, 136101 (2002).
- [29] Ş.C. Bădescu, K. Jacobi, Y. Wang, K. Bedürftig, G. Ertl, P. Salo, T. Ala-Nissila, and S.C. Ying, *Phys. Rev. B* **68**, 205401 (2003).
- [30] P. Légaré, *Surf. Sci.* **559**, 169 (2004).
- [31] D.C. Ford, Y. Xu, and M. Mavrikakis, *Surf. Sci.* **587**, 159 (2005).
- [32] F. Faglioni and W.A. Goddard, *J. Chem. Phys.* **122**, 014704 (2005).
- [33] S. Hong, T.S. Rahman, R. Heid, and K.P. Bohnen, *Phys. Rev. B* **71**, 245409 (2005); *Surf. Sci.* **587**, 41 (2005).
- [34] J. Fearon and G.W. Watson, *J. Mater. Chem.* **16**, 1989 (2006).
- [35] A.T. Gee, B.E. Hayden, C. Mormiche, and T.S. Nunnay, *J. Chem. Phys.* **112**, 7660 (2000); *Surf. Sci.* **512**, 165 (2002).
- [36] R.A. Olsen, Ş.C. Bădescu, S.C. Ying, and E.J. Baerends, *J. Chem. Phys.* **120**, 11852 (2004).
- [37] R.A. Olsen, D.A. McCormack, and E.J. Baerends, *Surf. Sci.* **571**, L325 (2004).
- [38] C.Z. Zheng, C.K. Yeung, M.M.T. Loy, and X. Xiao, *Phys. Rev. B* **70**, 205402 (2004).
- [39] M. Luppi, D.A. McCormack, R.A. Olsen, and E.J. Baerends, *J. Chem. Phys.* **123**, 164702 (2005).
- [40] D.A. McCormack, R.A. Olsen, and E.J. Baerends, *J. Chem. Phys.* **122**, 194708 (2005).
- [41] J. Ludwig, D.G. Vlachos, A.C.T. van Duin, and W.A. Goddard, *J. Phys. Chem. B* **110**, 4274 (2006).
- [42] C.Z. Zheng, C.K. Yeung, M.M.T. Loy, and X. Xiao, *Phys. Rev. Lett.* **97**, 166101 (2006).
- [43] R.A. Olsen, D.A. McCormack, M. Luppi, and E.J. Baerends, *J. Chem. Phys.* **128**, 194715 (2008).
- [44] I.M.N. Groot, K.J.P. Schouten, A.W. Kleyn, and L.B.F. Juurlink, *J. Chem. Phys.* **129**, 224707 (2008).
- [45] G. Kresse and J. Hafner, *Phys. Rev. B* **47**, 558 (1993); G. Kresse and J. Furthmüller, *Comput. Mater. Sci.* **6**, 15 (1996); G. Kresse and J. Furthmüller, *Phys. Rev. B* **54**, 11169 (1996).
- [46] J.P. Perdew, in *Electronic Structure of Solids '91*, edited by P. Ziesche and H. Eschring (Academic Verlag, Berlin, 1991).
- [47] G. Kresse and D. Joubert, *Phys. Rev. B* **59**, 1758 (1999).
- [48] H. Monkhorst and J. Pack, *Phys. Rev. B* **13**, 5188 (1976).
- [49] M. Methfessel and A.T. Paxton, *Phys. Rev. B* **40**, 3616 (1989).
- [50] N.W. Ashcroft and N.D. Mermin, *Solid State Physics* (Saunders, 1976).
- [51] <http://www.webelements.com/>
- [52] <http://fyslab.tkk.fi/epm/surfaces/hpt/>
- [53] P.M. Morse, *Phys. Rev.* **34**, 57 (1929).
- [54] Ş.C. Bădescu, P. Salo, T. Ala-Nissila, and S.C. Ying (unpublished).
- [55] J.P. Perdew, K. Burke, and M. Ernzerhof, *Phys. Rev. Lett.* **77**, 3865 (1996).
- [56] D. Vanderbilt, *Phys. Rev. B* **41**, 7892 (1990).
- [57] H. Jónsson, G. Mills, K.W. Jacobsen, in: *Classical and Quantum Dynamics in Condensed Phase Simulations*, Eds. B. J. Berne, G. Ciccotti, and D. F. Coker (World Scientific, Singapore, 1998); G. Mills, H. Jónsson, *Phys. Rev. Lett.* **72**, 1124 (1994); G. Mills, H. Jónsson, G. Schenter, *Surf. Sci.* **324**, 305 (1995).